Science and Technology Indonesia
e-ISSN:2580-4391 *p*-ISSN:2580-4405
Vol. 8, No. 3, July 2023

Review Paper

Dynamics of Extreme Rainfall and Its Impact on Forest and Land Fires in the Eastern Coast of Sumatra

Hamdi Akhsan[1], Muhammad Irfan[2], Supari[3], Iskhaq Iskandar[4]*

[1]*Department of Physics Education Faculty of Teaching and Education, Sriwijaya University, Indralaya, 30139, Indonesia*
[2]*Department of Physics Faculty of Mathematics and Natural Sciences, Sriwijaya University, Indralaya, 30139, Indonesia*
[3]*Indonesia Agency for Meteorology, Climatology and Geophysics (BMKG), Jakarta, 10610, Indonesia*
[4]*Graduate School of Sciences, Faculty of Mathematics and Natural Sciences, Sriwijaya University, Indralaya, 30139, Indonesia*
***Corresponding author**: iskhaq@mipa.unsri.ac.id

Abstract
This article examines the extreme climate events on the Eastern Coast of Sumatra over four decades (1981-2019) based on the extreme rainfall index defined using the Expert Team on Climate Change Detection and Indices (ETCCDI). The indices used include Consecutive Dry Day (CDD and the total rainfall per year (PRCPTOT). Theses indices were calculated and are based on the daily observation data from eight quality-controlled weather stations. While overall trends in extreme rainfall indices are not significant, there is a noticeable trend towards drought, with CDD rising by 1.23 days per decade and PRCPTOT decreased by 3.16 mm/year. The correlation between the Dipole Mode Index (DMI) and extreme rainfall indices in the August-September-October-November (ASON) period was positive, with CDD increasing with the more positive DMI value. On the other hand, the PRCPTOT index showed a decrease as the DMI more positive. The ENSO index and CDD are positively correlated during the dry season, while ENSO index negatively correlates with PRCPTOT. The duration of CDD during El Niño/positive Indian Ocean Dipole (IOD) events in 1997, 2015, and 2019 had significant impact on the forest and land fires on the Eastern Coast of Sumatra. The results are useful for policymakers in preventing forest and land fires on the Eastern Coast of Sumatra.

Keywords
Eastern Coast of Sumatra, El Niño-Southern Oscillation (ENSO), Extreme Rainfall Index, Forest and Land Fires, Indian Ocean Dipole

Received: 10 March 2023, Accepted: 12 June 2023
https://doi.org/10.26554/sti.2023.8.3.403-413

1. INTRODUCTION

The Northwest and Southeast Monsoon offer dynamic seasonal weather and rainfall in Indonesia. The rainy season occurs during the Northwest Monsoon period (December to March), while drier condition emerges during the Southeast Monsoon period (June-September). Previous study has proposed three patterns of the Indonesian rainfall, namely the equatorial pattern, the monsoonal pattern, and the local pattern (Aldrian and Dwi Susanto, 2003). The equatorial pattern has two peaks of rainy season occurring in October–November and March-May, while the monsoonal pattern shows seasonal variation with peak rainy season in November-February and peak dry season occurring in July-September. On the other hand, the local pattern shows a peak rainy season in June-July, in contrast to that of the monsoonal pattern.

However, at particular times the disturbances affect precipitation patterns due to changes in the monsoon wind pattern. These disturbances periodically appear interannually, originating from the ocean and atmosphere interaction in either the Pacific, called the El Niño Southern Oscillation (ENSO) (Philander, 1989) or the Indian Ocean anointed as the Indian Ocean Dipole (IOD) (Saji et al., 1999; Webster et al., 1999; Murtugudde et al., 2000). Both ENSO and IOD significantly affect precipitation patterns in Indonesia. Lack of precipitation arises due to ENSO warm phase or positive IOD, whereas ENSO cold phase or negative IOD produces above-average rainfall (Aldrian and Dwi Susanto, 2003; Hendon, 2003; Saji, 2001; Yamagata et al., 2004; Juneng and Tangang, 2005; Iskandar et al., 2018; Lestari et al., 2018; Utari et al., 2020). In addition, the study conducted by Siswanto et al. (2016) highlights the extreme rainfall in Jakarta during ENSO and IOD. This study found that ENSO and IOD are highly correlated to the precipitation in Jakarta, specifically during the dry season (June-November), but the correlation is insignificant during the rainy season (Lestari et al., 2019). Another research by Supari et al. (2017) investigates extreme rainfall and weather in Indonesia. They argue that extreme rainfall generates a wet-

ter condition. This study reveals that the average daily rainfall intensity dramatically increased around 0.21 mm/day, between 1983 and 2012.

Despite the considerable impact of weather and climate extremes, fewer studies have investigated globally ENSO-induced extremes than mean and seasonal climates. Alexander et al. (2009) discovered a link between global precipitation extremes and ENSO, but the impacts were different across regions, and there is a demand for a more specific investigation. Furthermore, Kenyon and Hegerl (2010) found a similar result where ENSO and extreme precipitation correlate substantially. On the other hand, Supari et al. (2018) indicate that the impact of El Niño is prominent during arid conditions in Sumatra, specifically in June-July-August (JJA) and September-October-November (SON). Further, a wet anomaly occurs in Eastern Sumatra in December-January-February (DJF) and March-April-May (MAM), creating a disparity of wetness on the island.

The impacts of ENSO and IOD strongly link to forest and land fires (Nur'utami and Hidayat, 2016). Historically, forest and land fires in Indonesia have become a big concern due to their massive impacts. The impacts of forest and land fires spread widely across the sectors, including social, health, education, and economy, particularly in the Sumatra, Kalimantan, and Papua regions, with the largest forest areas (Edwards and Heiduk, 2015; Purnomo et al., 2017). Burton et al. (2020) analyze the impacts of En Niño on burned areas and carbon sinks. The finding suggests that El Niño conditions positively correlate with higher burned areas in most regions. This study also emphasizes that El Niño caused a 4% enlargement of burned area and a 5% increase in carbon emission compared to a non-El Niño scenario. Similarly, a study by Prasetyo et al. (2022) using a machine learning technique observes that the peatland vulnerability to fire increases during El Nino conditions. Although previous research has extensively investigated rainfall patterns and extreme weather in Indonesia, there is a demand for a study investigating El Niño on the Eastern Coast of Sumatra, including research on rainfall dynamics, extreme events, and their relationship to climate anomalies. Prior studies show that the Eastern Coast of Sumatera is dominated by peatland and highly vulnerable to climate anomalies (Worden et al., 2013; Huijnen et al., 2016; Putra et al., 2019b; Putra et al., 2019a)

This research examines the relationship between extreme rainfall and El Niño-Southern Oscillation (ENSO) and the Indian Ocean Dipole (IOD) and their impacts on sparking forest and land fires on the Eastern Coast of Sumatra. In addition, this study also identifies possible changes in the time series based on the F-test approach (Wang and Feng, 2013). This study will contribute to academia by shedding light on the interplay of climatological parameters. Furthermore, this research may guide the Indonesian government in creating strategies to prevent forest and land fires on the Eastern Coast of Sumatra.

2. EXPERIMENTAL SECTION

This research uses the rain gauge and temperature measuring instruments at BMKG weather stations in the Eastern Coastal area of Sumatra, covering six provinces: Lampung, South Sumatra, Jambi, Riau, Riau Island, and Bangka Belitung Island (Figure 1). Province, Station name, latitude, longitude and elevation at Table 1.

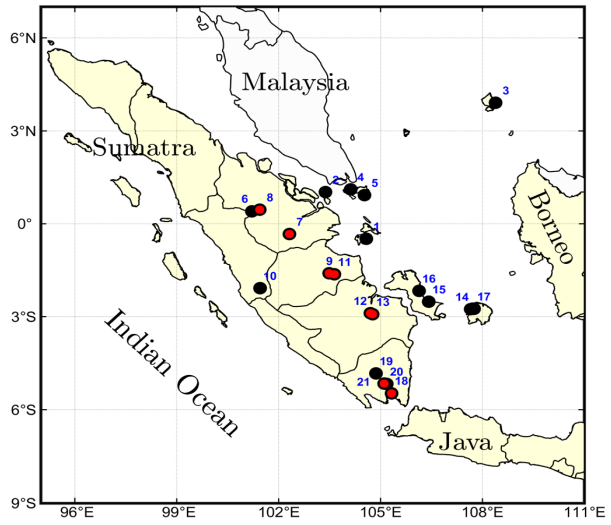

Figure 1. Spatial Distribution of 21 Tested Stations (Red Dots Represent Selected Stations)

We filtered data from 21 stations through quality control (QC). A quality control procedure is helpful to determine and identify any errors during data collection. Regarding temperature data, Stooksbury et al. (1999) emphasize that missing or unrecorded temperature values in the data used can significantly impact trend analysis. Therefore, quality control of the data is necessary to identify extreme temperatures. This QC evaluation only examines data that contains at least 80% of full years. A full year describes a complete record of data with a maximum of only 15 unrecorded days and without three consecutive days of missing data (Aguilar et al., 2009; Supari et al., 2017; Supari et al., 2018). During long-term temperature observation, unusual temperature shifts are common due to ENSO and IOD anomalies, including technical factors such as environment changeability around the observation point, relocation of measurement tools, and human error (Tank et al., 2009; Supari et al., 2017). This notion indicates the importance of quality control as a preliminary stage of this study.

2.1 Data and Procedures

2.1.1 Data on Rainfall

The research was conducted in four stages: 1) Data collection, quality control, and homogeneity analysis; 2) calculation of extreme rainfall; 3) Trend detection and analysis using Mann-Kendall and Sens slope tests; and 4) Final interpretation.

Table 1. Preliminary List of Stations

No.	Name	Province	Latitude	Longitude	Elevation
1	SM Dabo	Riau Islands	-0.480	104.580	29
2	SM Raja Haji Abdullah	Riau Islands	1.030	103.380	1
3	SM Ranai	Riau Islands	3.912	108.390	2
4	SM Hang Nadim	Riau Islands	1.117	104.117	26
5	SM Raja Haji Fisabilillah	Riau Islands	0.923	104.529	15
6	SK Kampar	Riau	0.407	101.217	15
7	SM Japura	Riau	-0.330	102.320	19
8	SM Sultan Syarif Kasim II	Riau	0.459	101.447	39
9	SK Muaro Jambi	Jambi	-1.602	103.484	24
10	SM Depati Parbo	Jambi	-2.083	101.450	782
11	SM Sultan Thaha	Jambi	-1.634	103.640	26
12	SM Sultan Mahmud Badaruddin II	South Sumatra	-2.895	104.701	10
13	SK Palembang	South Sumatra	-2.927	104.772	11
14	SG Tanjung Pandan	Bangka Belitung Islands	-2.758	107.650	22
15	SK Bangka Tengah	Bangka Belitung Islands	-2.518	106.422	6
16	SM Depati Amir	Bangka Belitung Islands	-2.170	106.130	0
17	SM H. AS. Hananjoeddin	Bangka Belitung Islands	-2.750	107.750	50
18	SMM Panjang	Lampung	-5.472	105.321	7
19	SG Lampung Utara	Lampung	-4.836	104.870	60
20	SK Pesawaran	Lampung	-5.172	105.180	71
21	SM Raden Inten II	Lampung	-5.160	105.110	85

2.1.2 Data on Forest and Land Fires

Data on forest and land fires in four provinces (Riau, Jambi, South Sumatra, and Lampung) was obtained from the official website of the Ministry of Environment and Forestry (https://sipongi.menlhk.go.id/). The data (Table 2) shows the extent of burned land and forests over the past 25 years (1997-2022).

2.1.3 ENSO and IOD Index Data

ENSO index was obtained conventionally by calculating the Southern Oscillation Index (SOI) value. which represents the strength of Walker circulation. Then. we calculated ENSO evolution through sea surface temperature (SST) anomaly analysis in several equatorial regions in the Pacific Ocean (Niño region): Niño1+2, Niño3, Niño4, and Niño3.4. We collected the data of Niño3.4 for the ENSO index as Niño3.4 correlates with the Indonesian precipitation pattern. Niño3.4 region is located in 5° S-5° N. 170°-120° W astronomical coordinates. Similar to El Niño. Indian Ocean Dipole (IOD) describes the sea surface temperatures disparity of the West Indian Ocean (50°-70° E dan 10° S - 10° N) and East Indian Ocean (90°-110° E dan 10° S - 0° N). The disparity index for this phenomenon is Dipole Mode Index (DMI). Positive DMI indicates that the sea surface temperature in the East Indian Ocean is colder than in the West Indian Ocean.

2.2 Calculations for the Rainfall Index

The rainfall index measurement involves intensity. duration. and extreme frequency. This study utilizes the RClimDex software to measure extreme rainfall and calculate the index (Zhang and Yang, 2004) as shown in Table 3.

2.3 Trend Detection and Analysis using the Mann-Kendall and Sens Slope Tests

This research employs a non-parametric Mann-Kendall (MK) test for detecting trends in a set of hydrological data (WMO, 2018). confluence with Sen's slope estimator to evaluate the trend of indices. The MK test is indispensable to assessing the statistical significance of the trend and Sen's slope estimator is essential to quantify the magnitude of the trend. This methodology is well-known for analyzing climate data because of its robustness against outliers and its non-reliance on the assumption of normality (Zhang et al., 2005; Vincent et al., 2011; Keggenhoff et al., 2014). This rank-based technique is less sensitive to missing data, with a 95% significance level.

Table 2. Forest and Land Fires Data at Four Provinces in Sumatra

Year\Province	Jambi	Lampung	Riau	South Sumatra	Total Burned Area
1997	6,150.27	21,311.17	4,063.88	34,299.88	65,825.20
1998	0.00	0.00	579.00	19.00	598.00
1999	1,087.50	7,378.25	852.00	0.00	9,317.75
2000	21.00	10.00	0.00	0.00	31.00
2001	30.00	0.00	422.35	7,868.92	8,321.27
2002	212.00	7,137.30	2,211.85	10,983.53	20,544.68
2003	3,025.00	0.00	7.50	233.00	3,265.50
2004	138.40	0.00	0.00	953.00	1,091.40
2005	67.00	0.00	0.00	0.00	67.00
2006	1,726.80	0.00	1,106.70	1,726.00	4,559.50
2007	81.00	2,532.25	89.75	41.00	2,744.00
2008	114,52	2.956,00	109,00	84,00	3.263,52
2009	14.00	0.00	275.30	51.00	340.30
2010	2.50	106.00	26.00	0.00	134.50
2011	89.00	31.00	74.50	84.50	279.00
2012	11.25	0.00	1.060.00	0.00	1.071.25
2013	199.10	0.00	1,077.50	484.15	1,760.75
2014	3,470,605.00	22.80	6,301.10	8,504.86	3,485,433.76
2015	115,634.34	71,326.49	183,808.59	646,298.80	1,017,068.22
2016	8,281.25	3,201.24	85,219.51	8,784.91	105,486.91
2017	109.17	6,177.79	6,866.09	3,625.66	16,778.71
2018	1,577.75	15,156.22	37,236.27	16,226.60	70,196.84
2019	56,593.00	35,546.00	90,550.00	336,798.00	519,487.00
2020	1,002.00	1,358.00	15,442.00	950.00	18,752.00
2021	540.00	5,411.00	8,970.00	5,245.00	20,166.00
2022	918.00	7,989.00	4,915.00	3,723.00	17,545.00
Total	442,020.61	188,637.49	1,212,820.68	151,813.79	2,043,088.67

2.4 Correlation Analysis Between Extreme Rainfall with Climate Indices and Hotspots in the Eastern Coast of Sumatra

We analyze the correlation between extreme rainfall indices and ENSO and IOD at this stage. This correlation analysis is the key to determining the influence of ENSO and IOD on the extreme temperatures on the Eastern Coast of Sumatra. The final result of the correlation analysis will be compared to the data on land fires. particularly during extreme land fire incidents in El Nino and positive IOD years, in 1997, 2015, and 2019.

3. RESULTS AND DISCUSSION

3.1 Result and Findings

3.1.1 Data Quality Control

This study obtained initial analysis from rainfall. ranging from 4-40 years of data records of 21 BMKG stations in Sumatra through the BMKG website (www.bmkg.online). Further, we selected 8 stations with data over 20 years (Table 4). Manual quality control procedures were employed to detect and identify errors. This study only utilized data from observation stations with at least 80% full years. Data from www.meteomanz.id accompanied the data obtained from the website www.bmkg.online. After the manual QC procedure, 8 BMKG stations on the Eastern Coast of Sumatra are qualified to undergo the second-stage QC procedure.

The main purpose of the second quality control stage is to relinquish the error in the observational data (the data works beyond the interquartile range. IQR) for outlier detection. All data were obtained through RClimedex Extra QC software, IQR, lower limit, and upper limit for each month's data were calculated based on observational data each year. The data above the upper limit or below the lower limit are considered outliers, which later be normalized using the RH test.

3.1.2 Extreme Precipitation Index

This research selects and 2 rainfall indices of Indonesia. The rainfall indices capture the intensity, duration, and frequency of extremes. The index calculations rely on both the station and global threshold levels. The specific requirements are mandatory to compute index value using RClimDex 1.0. The monthly index cannot have missing data for more than three days. while the annual index excludes only 15 days. In addition. the threshold is calculated if data is available at least 70% of the total data. The analyzed data comprises Consecutive Dry Days

Table 3. Extreme Rainfall Index used in This Study

ID	Indicator Name	Indicator Definition
PRCPTOT	Annual total wet-day precipitation	Annual total precipitation from days ≥ 1 mm
CDD	Consecutive dry days	Maximum number of consecutive days when precipitation < 1 mm

Table 4. Locations of Selected Stations

Number before QC	Number post QCo	Station Name	Latitude	Longitude	Range
13	1	SK Palembang	-2.93	104.77	1981-2020
12	2	SM Sultan Mahmud Badaruddin II	-2.89	104.70	1981-2020
9	3	SK Muaro Jambi	-1.60	103.48	1997-2020
11	4	SM Sultan Thaha	-1.63	103.64	1985-2019
7	5	SK Japura Rengat	-0.33	102.32	1982-2020
8	6	SM Sultan Syarif Kasim II	0.45	101.44	1981-2020
18	7	SMM Panjang	-5.47	105.32	1998-2020
21	8	SM Raden Intan II	-5.16	105.11	1981-2020

Table 5. Trends for Consecutive Dry Day at 8 Rainfall Stations in the Eastern Coast of Sumatra

Station	Trend	P Value
SK Palembang Sta01	0.23	0.37
SM Sultan Mahmud Badaruddin II Sta02	0.23	0.37
SK Muaro Jambi Sta03	0.01	0.99
SM Sultan Thaha Sta04	0.32	0.34
SK Japura Rengat Sta05	0.16	0.43
SM Sultan Syarif Kasim II Sta06	0.11	0.31
SMM Panjang Sta07	0.03	0.75
SM Raden Intan II Sta08	0.04	0.93
Avarage	0.12	0.26

(CDD) and Annual Total Precipitation (PRCPTOT).

The first extreme rainfall index reviewed is the CDD in eight BMKG stations located in four southern provinces of Sumatra. The observed data trend per station is shown in Table 5.

Based on data from eight observation stations. there was a consistent rise in the number of CDDs across all locations. No negative trend in the total dry days was observed in the eight stations. Similar findings were reported by Muhammad et al. (2020) in their research conducted in Malaysia. The highest upsurge in CDD was observed in SK Muaro Jambi Station. followed by SK Palembang and SMB II Meteorological Station. The lowest increase was observed in SM SSK II Station. The overall increase in the duration of CDD is (1.23 ± 2.6) days per decade. The trend details for spatial data of CDD are shown in Figure 2.

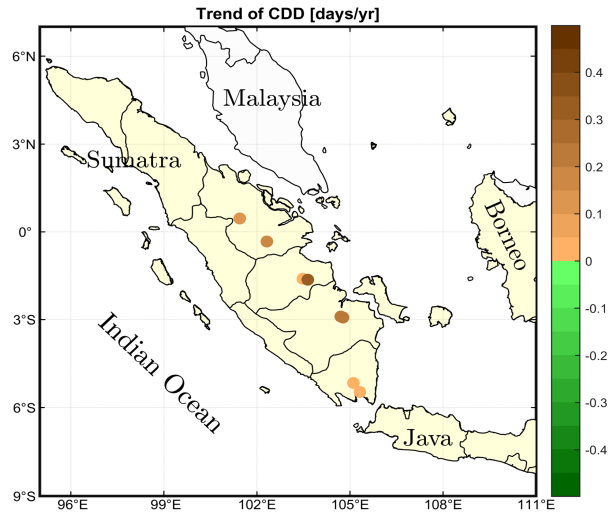

Figure 2. Spatial Distribution of CDD Trend in Selected Stations

The second extreme rainfall index reviewed was PRCPTOT for eight BMKG stations in 4 Eastern Coast of Sumatra provinces. The observed PRCPTOT data trend per stations is presented in Table 6.

From the Table 6, the highest PRCPTOT data was recorded at SMM Panjang Station; the greatest reduction was observed at SM Raden Intan II Station. The distinctive trends between the two stations need to investigate further. The decrease in total precipitation for one year. -3.2 ± 7.2 mm per decade,

Table 6. Trends for Total Precipitation at 8 Rainfall Stations in the Eastern Coast of Sumatra

Station	Trend	P Value
SK Palembang	2.68	0.71
SM Sultan Mahmud Badaruddin II	0.75	0.91
SK Muaro Jambi	-3.64	0.79
SM Sultan Thaha	-0.144	0.01
SK Japura Rengat	-0.78	0.88
SM Sultan Syarif Kasim II Sta06	5.82	0.40
SMM Panjang Sta07	7.544	0.55
SM Raden Intan II Sta08	-9.70	0.15
Average	-0.32	0.72

indicates a gradual loweris in total rainfall over the four decades. This phenomenon also occurred in Iran, as demonstrated in research conducted by Noorisameleh et al. (2020). This phenomenon may be attributed to infrequent yet precipitation events. Figure 3 represents the special PRCPTOT trend each station.

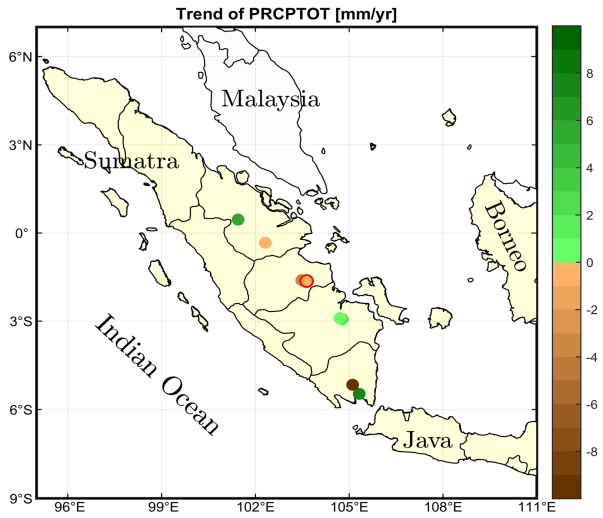

Figure 3. Spatial Distribution of PRCPTOT Trend in Selected Stations

This study scrutinized two indices at eight observation stations in South Sumatra, Jambi, Riau, and Lampung. Table 7 shows CDD indices are increasing and one is plunging. Dry days are increasing while rainy days are declining. Total annual rainfall is descending. with intense rainfall lowering every decade. This trend is supported by other studies conducted in the Western United States, Brazil, and India (Zhang et al., 2021; Mishra, 2019).

3.1.3 Correlation of Extreme Rainfall with ENSO

The purpose of this study is to analyze the correlation between two extreme rainfall indices (CDD and PRCPTOT) and two

Table 7. Trend for the Overall Extreme Rainfall Index

Indeks	Highest Trend	Lowest Trend	Total	Average
PRCPTOT	7.544	-9.70	2.53	-0.32
CDD	0.321	0.01	0.99	0.12

Table 8. Critical Correlation for One Tile Pearson Correlation

df = N-2	0.1 *	0.05 **	0.025 ***	0.01 ****
18	0.30	0.38	0.44	0.52
20	0.28	0.38	0.42	0.49
34	0.23	0.28	0.33	0.39
35	0.22	0.28	0.324	0.38
37	0.22	0.28	0.32	0.37
38	0.22	0.27	0.31	0.37

climatic phenomena (ENSO and IOD). The DMI and ENSO index data are mandatory to analyze the correlation between extreme rainfall indices and ENSO. We moderated the DMI data over 40 years and 12 months (1981-2020). This study calculated the significant level of each index's connection using confidence levels of 10% (low), 5% (adequate), 2.5% (high), and 1% (very high). denoted by asterisk (*) in Table 8 below. This study used monthly averages to investigate the correlation between the DMI index and the extreme rainfall index. The strongest correlation was observed during August, September, October, and November (ASON). The Pearson one-tile correlation uses the R-ASON value as a benchmark for statistical significance. The exact correlation values are presented as follows:

The correlation between the ENSO index and extreme rainfall index was investigated using three earlier calculations of monthly average variations for the DMI average index. One tile of the person correlation coefficient was utilized to observe the relationship between the monthly average ENSO index and extreme rainfall index, resulting in the following values:

Table 9 presents the findings of this study based on data from eight stations. It shows that the highest correlation between the average ENSO index and extreme rainfall index occurs during August, September, October, November (ASON) for measures of CDD and total precipitation (PRCPTOT) was used to calculate the Pearson One-Tile correlation significance. The results show a high significance level for the SM Sultan Thaha Station and significant levels for SM Palembang and the SM Sultan Mahmud Badaruddin II and SM Raden Intan II station. However, the correlation coefficient for the SK Muaro Jambi station is low. There is no significant relationship between the two variables for the SK Japura Rengat, SM Sultan Sarif Kasim II, and SMM Panjang station.

The correlation between the ENSO index and CDD is

Table 9. Correlation Coefficients of ENSO and the Extreme Precipitation Index

	CDD							
	Sta01	Sta02	Sta03	Sta04	Sta05	Sta06	Sta07	Sta08
N (years)	38	38	18	34	37	35	20	38
r	0.64****	0.62****	0.55****	0.57****	0.57****	0.01*	0.39***	0.57****
	PRCPTOT							
	Sta01	Sta02	Sta03	Sta04	Sta05	Sta06	Sta07	Sta08
N (years)	38	38	18	34	37	35	20	38
r	- 0.51****	- 0.59****	-0.55****	- 0.53****	-0.33***	0.26*	-0.19	-0.51****

Note: ****significant at 1% alpha, *** significant at 2.5% alpha, ** significant at 5% alpha, *significant at 10% alpha

very significant for data from the SK Palembang, SM Sultan Mahmud Badaruddin II, SK Muaro Jambi, SM Sultan Thaha, SK Japura Rengat, and SM Raden Intan II Station. The correlation is significant for the SMM Panjang Station but not for SM Sultan Syarif Kasim II data. The correlation between ENSO index and the total rainfall in one year (PRCPTOT) has a very high level of significance for observation data from SK Palembang. SM Sultan Mahmud Badaruddin II, and SM Sultan Thaha Station, and a significant level of significance for SK Japura Rengat and SM Raden Intan II Station. The correlation is significant at a weak degree for SK Muaro Jambi and SM SSK II Station. while the correlation is quite significant for SMM Panjang Station. The Pearson correlation test for the relationship between the ENSO Index and the extreme rainfall index shows a high level of significance for the SM Sultan Thaha Station, a moderate level for the SK Japura Rengat Station. and a weak level for the SK Palembang, SK Muaro Jambi, and SM SSK II Station. However, the correlation is insignificant for the SM SMB II and SMM Panjang Station. Overall, ENSO has significant contribution to the CDD and PRCPTOT index. It contributes to less rain at the observed points.

3.1.4 Correlation of Extreme Rainfall with the Indian Ocean Dipole (IOD)

DMI data are mandatory to analyze the correlation between extreme rainfall indices and IOD. Similar to the previous stage. we moderated the 40 years and 12 months (1981-2020) DMI data. This also research determined the significance level of the correlation of each index by using confidence degrees of 10% (low), 5% (sufficient), 2.5% (high), and 1% (very high), denoted by (*) in Table 10 below.

Based on the results in Table 10. there is a substantial correlation between DMI and CDD for data from SK Palembang, SM Sultan Mahmud Badaruddin II, and SK Muaro Jambi Stations. A considerable correlation is found in the observation data at the SK Japura Rengat, SMM Panjang, and SM Raden Intan II Stations. Only the SM Sultan Syarif Kasim II Station shows an insignificant correlation. Our results show notable correlations at deviating levels across various stations. Data from SK Palembang, SM Sultan Mahmud Badaruddin II, and SM Sultan Taha Stations show a highly significant correlation. SK Japura Rengat and SM Raden Intan II Stations also exhibit high significance. commensurate to previous research by Lestari et al. (2019) in Jakarta. The SMM Panjang station shows moderate significance, while the SM Muaro Jambi and SM Sultan Syarif Kasim II have weak correlations.

The Pearson correlation coefficient test results show a high significance between DMI and the Extreme Rainfall Index for the SM Sultan Taha. sufficient significance for the SK Japura Rengat, and weak significance for SM Sultan Mahmud Badaruddin II, SM Muaro Jambi, and SM Sultan Syarif Kasim II Stations. However, there is no significant correlation at the SM Sultan Mahmud Badaruddin II, SMM Panjang, and SM Raden Intan II Stations.

The Pearson correlation coefficient test results show a high significance between DMI and the Extreme Rainfall Index for the SM Sultan Taha Station, sufficient significance for the SK Japura Rengat Station, and weak significance for SK Palembang. SK Muaro Jambi, and SM Sultan Syarif Kasim II Stations. However. there is no significant correlation at the SM Sultan Mahmud Badaruddin II, SMM Panjang, and SM Raden Intan II Stations. Overall, similar to ENSO, IOD has significant contribution to the CDD and PRCPTOT index. It also influences the deficit rainfall at the observed points.

3.1.5 Forest and Land Fires in Four Provinces in the Eastern Coast of Sumatra

Data over 25 years shows extensive forest and land fires in 1997, 2015, and 2019 (Table 11). In 1997, a widespread series of forest fires in Indonesia threw a blanket of thick, smoky haze over a large portion of Southeast Asia. The smoke covered most of Southeast Asia nations and persisted for several months (Sastry, 2002). The fires destroyed a huge amount of rainforest and contributed to a significant release of greenhouse gases. In 2015, the cumulative area of forest and land fires in the four sampled provinces accounted for 19% of the total area affected by such fires over 25 years. In 2019, the El Niño occurred during the first semester of the year and IOD occurred in the second semester. There is a proof that in 2019. IOD was strong, preceded by a weak El Niño (Iskandar et al., 2022). Both El Niño and IOD occurred at the different

Table 10. Correlation Coefficients of DMI and the Extreme Precipitation Index

Indicator	Sta01	Sta02	Sta03	Sta04	Sta05	Sta06	Sta07	Sta08
df=N-2	38	38	19	34	37	33	21	38
R CDD	0.69****	0.72****	0.65****	0.61****	0.57***	0.16	0.72***	0.74***
R PRCPTOT	-0.57****	-0.53****	-0.36*	-0.52****	-0.42***	-0.39***	-0.46**	-0.54***

time. The El Nino phenomenon is categorized into four levels based on anomalous sea surface temperature (SST): Weak (0.5-0.9 SST anomaly), Moderate (1-1.4 SST anomaly), Strong (1.5-1.9 SST anomaly), and Very Strong (greater than 2 SST anomaly) (elnino.noaa.gov). The following table compares 1997, 2015, 2019 El Niño years with the number of CDD and the extent of land fires for available data years.

3.1.6 Prediction and Projection of Forest and Peatland Fires in Eastern Coast of Sumatra Related to Extreme Rainfall

Based on the results of statistical data processing on the extreme climate index in the four provinces of the Eastern Coast of Sumatra. Figure 4 and 5 show the combined trends detected for the two extreme climate indicators.

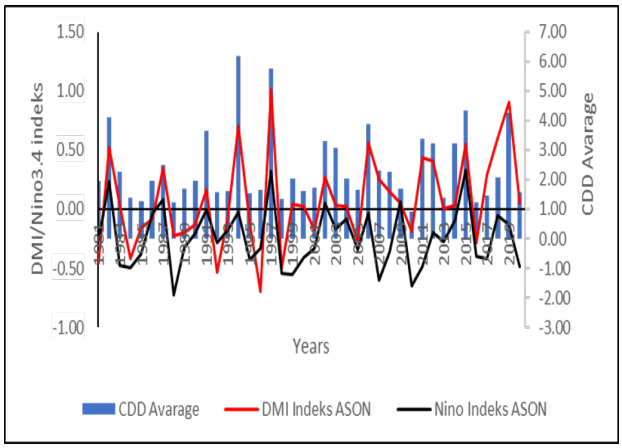

Figure 4. Average CCD for All Stations. DMI/ENSO Index

Figure 4 shows an increasing trend in CDD and a decreasing trend in Annual total wet-day precipitation (PRCPTOT) on the Eastern Coast of Sumatra. These results suggest that the region is becoming drier with a rise in mean temperature during day and night. This occurrence could lead to an expansion of susceptible land and forests vulnerable to wildfires. This projection aligns with a previous study by Supari et al. (2018) that predicted changes in annual precipitation extremes over Southeast Asia with 2°C global warming by 2041. Figure 6 indicates the increasing trend of wildfires in the area of Eastern Coast of Sumatra.

The graph shows relationship consistency between burned land area combined with the rise in CDD, ENSO Index, and IOD index. Using a case study approach. this study investi-

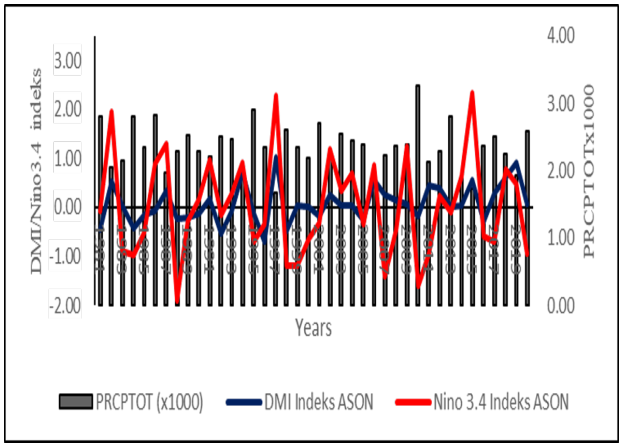

Figure 5. PRCPTOT for All Stations DMI/ENSO Index in Four Provinces Located in the Eastern Coast of Sumatra

gates land fires in four provinces (Riau, Jambi, South Sumatra, and Lampung) between 2015 and 2019. It explores the relationship between land fires and three climatic indices: the Dipole Mode Index (DMI), the El Niño-Southern Oscillation (ENSO) index in the ENSO region, and the number of CDD. Available data for these years are used to analyze the extent of burned area and its correlation with the climatic indices. Overall, this study suggests that forest and land fires incident positively correlate with ENSO/IOD occurrence.

From September to December 2015, the mean value of the ENSO index was 2.57, peaking at 2.56 in December. This value corresponds with a DMI of 0.567 and 43.63 consecutive dry days (CDD). That year, the total burned area was extensive at 1.017.068.22 hectares, accounting for 54% of the total burned area recorded over 23 years. In 2019, despite a weak Nino index and Strong IOD, the burned area remained vast (Iskandar et al., 2022). In 2006, 2015, and 2019, areas with high-density hotspots (exceeding 51 points) were concentrated in the Eastern part of the Eastern Coast of Sumatra, characterized by peatlands. Peatlands dominate much of the land in the Eastern provinces of Riau, Jambi, South Sumatra, and Lampung. Figure 7 represents the hotspot density and distribution in Eastern Coast of Sumatra in 2015 and 2019

3.2 Discussion

This study implies a notable correlation between ENSO and DMI indices and the increasing trend in consistent dry days. Similarly. the research by Phuong et al. (2022) in Vietnam

Table 11. Categories of El Niño and IOD Events

Year	Highest ENSO	Highest DMI	CDD Average	Burned Land Area (ha)
1997	2.4	1.28	57.8	65.825.20
2015	2.57	0.57	43.6	1.017.068.22
2019	0.81*	0.89	42.6	519.487.00

*Note: El Niño in the first semester. IOD in the second semester

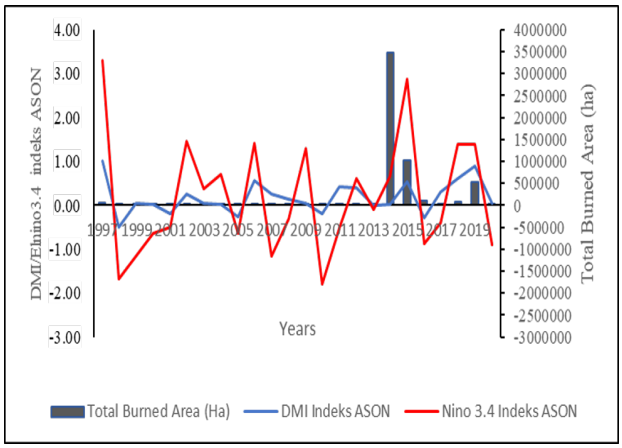

Figure 6. ENSO Index for ASON. DMI Index for ASON

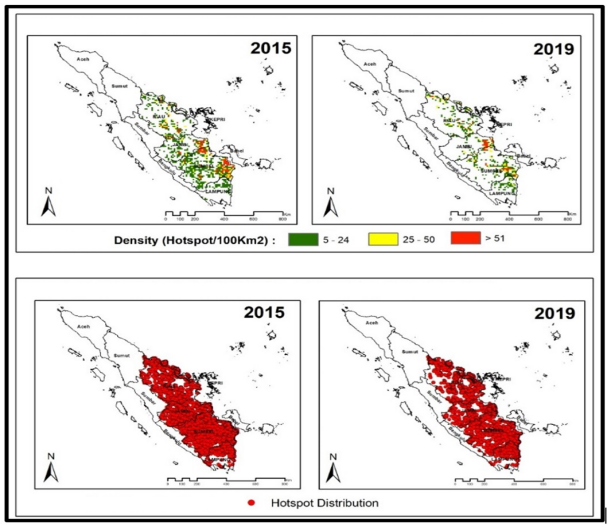

Figure 7. Hotspots Density (*Upper Panel*) and Distribution (*Lower Panel*) Observed in the Eastern Coast of Sumatra in 2015 and 2019

reported a significant correlation between CDD, the ENSO index, and DMI. This correlation means an increased number of hotspots and burned areas. The declining trend in wet days provides a fundamental root for policy making for forest and land fire mitigation on the Eastern Coast of Sumatra. During El Nino events and positive IOD phases, the number of rainless days is expected to increase, leading to higher forest and land drought conditions and a high risk of forest and land fires. This phenomenon has been observed in previous studies, such as in the Amazon, where Cochrane and Schulze (1999) and Ray et al. (2005) found increased land and forest flammability during the El Niño phases.

In summary, ENSO and IOD dynamics are critical in the Eastern Coast of Sumatra's weather patterns and significantly impact extreme rainfall and forest/land fires. Understanding these dynamics can assist policymakers in developing efficacious strategies to manage related hazards. These strategies may include fire suppression measures, evacuation preparedness, healthcare services, and other forest and land fire prevention measures such as deploying firefighting teams, disaster-ready volunteers on site, land canals, air-based fire suppression, constructing new reservoirs, maintaining existing reservoirs, and preparing firefighting equipment in disaster-prone areas.

4. CONCLUSION

This study found a significant correlation between the rise in ENSO indices and DMI indices and the increasing trend in consistent dry days on the Eastern Coast of Sumatra. During El Niño events and positive IOD phases, dry days increase, leading to higher forest and land drought conditions and an elevated risk of forest and land fires. The DMI index showed a positive correlation with the number of CDD and a negative correlation with the total amount of rainfall in one year. Similarly. the ENSO index showed a positive correlation with the number of CDD. The increase in CDD during El Nino events in 1997, 2015, and 2019 significantly impacted widespread forest and land fires on the Eastern Coast of Sumatra. These findings provide valuable insights for policymakers to develop effective strategies to manage related risks.

5. ACKNOWLEDGMENT

This study is part of the first author's dissertation. We thank the Agency of Mateorology, Climatology and Geophysics, Republik of Indonesia for providing the rain gauge data. We also thank two anonymuous reviewers for their constructive comments and suggestions. This study is supported by grant in aid for the last author from the Ministry of Education, Culture, Research and Technology, Republic of Indonesia.

REFERENCES

Aguilar, E., A. Aziz Barry, M. Brunet, L. Ekang, A. Fernandes, M. Massoukina, J. Mbah, A. Mhanda, D. Do Nascimento, T. Peterson, et al. (2009). Changes in Temperature and Precipitation Extremes in Western Central Africa, Guinea Conakry, and Zimbabwe, 1955–2006. *Journal of Geophysical Research: Atmospheres*, **114**(D2)

Aldrian, E. and R. Dwi Susanto (2003). Identification of Three Dominant Rainfall Regions within Indonesia and Their Relationship to Sea Surface Temperature. *International Journal of Climatology: A Journal of the Royal Meteorological Society*, **23**(12); 1435–1452

Alexander, L. V., P. Uotila, and N. Nicholls (2009). Influence of Sea Surface Temperature Variability on Global Temperature and Precipitation Extremes. *Journal of Geophysical Research: Atmospheres*, **114**(D18); 1–13

Burton, C., R. A. Betts, C. D. Jones, T. R. Feldpausch, M. Cardoso, and L. O. Anderson (2020). El Niño Driven Changes in Global Fire 2015/16. *Frontiers in Earth Science*, **8**; 199

Cochrane, M. A. and M. D. Schulze (1999). Fire as a Recurrent Event in Tropical Forests of the Eastern Amazon: Effects on Forest Structure, Biomass, and Species Composition[1]. *Biotropica*, **31**(1); 2–16

Edwards, S. A. and F. Heiduk (2015). Hazy Days: Forest Fires and the Politics of Environmental Security in Indonesia. *Journal of Current Southeast Asian Affairs*, **34**(3); 65–94

Hendon, H. H. (2003). Indonesian Rainfall Variability: Impacts of ENSO and Local Air–Sea Interaction. *Journal of Climate*, **16**(11); 1775–1790

Huijnen, V., M. J. Wooster, J. W. Kaiser, D. L. Gaveau, J. Flemming, M. Parrington, A. Inness, D. Murdiyarso, B. Main, and M. van Weele (2016). Fire Carbon Emissions Over Maritime Southeast Asia in 2015 Largest Since 1997. *Scientific Reports*, **6**(1); 1–8

Iskandar, I., D. Lestari, P. Utari, M. Khakim, P. Poerwono, D. Setiabudidaya, et al. (2018). Evolution and Impact of the 2016 Negative Indian Ocean Dipole. In *Journal of Physics: Conference Series*, volume 985. IOP Publishing, page 012017

Iskandar, I., D. O. Lestari, A. D. Saputra, R. Y. Setiawan, A. Wirasatriya, R. D. Susanto, W. Mardiansyah, M. Irfan, Rozirwan, and J. D. Setiawan (2022). Extreme Positive Indian Ocean Dipole in 2019 and Its Impact on Indonesia. *Sustainability*, **14**(22); 15155

Juneng, L. and F. T. Tangang (2005). Evolution of ENSO-Related Rainfall Anomalies in Southeast Asia Region and Its Relationship with Atmosphere–Ocean Variations in Indo-Pacific Sector. *Climate Dynamics*, **25**; 337–350

Keggenhoff, I., M. Elizbarashvili, A. Amiri-Farahani, and L. King (2014). Trends in Daily Temperature and Precipitation Extremes Over Georgia, 1971–2010. *Weather and Climate Extremes*, **4**; 75–85

Kenyon, J. and G. C. Hegerl (2010). Influence of Modes of Climate Variability on Global Precipitation Extremes. *Journal of Climate*, **23**(23); 6248–6262

Lestari, D. O., E. Sutriyono, S. Kadir, and I. Iskandar (2018). Respective Influences of the Indian Ocean Dipole and El-Niño-Southern Oscillation on the Indonesian Precipitation. *Journal of Mathematical and Fundamental Sciences*, **50**(3); 257–272

Lestari, S., A. King, C. Vincent, D. Karoly, and A. Protat (2019). Seasonal Dependence of Rainfall Extremes in and Around Jakarta, Indonesia. *Weather and Climate Extremes*, **24**; 100202

Mishra, A. K. (2019). Quantifying the Impact of Global Warming on Precipitation Patterns in India. *Meteorological Applications*, **26**(1); 153–160

Muhammad, N., J. Abdullah, and P. Julien (2020). Characteristics of Rainfall in Peninsular Malaysia. In *Journal of Physics: Conference Series*, volume 1529. IOP Publishing, page 052014

Murtugudde, R., J. P. McCreary Jr, and A. J. Busalacchi (2000). Oceanic Processes Associated with Anomalous Events in the Indian Ocean with Relevance to 1997–1998. *Journal of Geophysical Research: Oceans*, **105**(C2); 3295–3306

Noorisameleh, Z., S. Khaledi, A. Shakiba, P. Z. Firouzabadi, W. A. Gough, and M. M. Q. Mirza (2020). Comparative Evaluation of Impacts of Climate Change and Droughts on River Flow Vulnerability in Iran. *Water Science and Engineering*, **13**(4); 265–274

Nur'utami, M. N. and R. Hidayat (2016). Influences of IOD and ENSO to Indonesian Rainfall Variability: Role of Atmosphere-Ocean Interaction in the Indo-Pacific Sector. *Procedia Environmental Sciences*, **33**; 196–203

Philander, S. G. (1989). El Niño, La Niña, and the Southern Oscillation. *International Geophysics Series*, **46**; X–289

Phuong, D. N. D., N. T. Huyen, N. D. Liem, N. T. Hong, D. K. Cuong, and N. K. Loi (2022). On the Use of an Innovative Trend Analysis Methodology for Temporal Trend Identification in Extreme Rainfall Indices Over the Central Highlands, Vietnam. *Theoretical and Applied Climatology*; 1–18

Prasetyo, L. B., Y. Setiawan, A. A. Condro, K. Kustiyo, E. I. Putra, N. Hayati, A. K. Wijayanto, A. Ramadhi, and D. Murdiyarso (2022). Assessing Sumatran Peat Vulnerability to Fire under Various Condition of ENSO Phases Using Machine Learning Approaches. *Forests*, **13**(6); 828

Purnomo, H., B. Shantiko, S. Sitorus, H. Gunawan, R. Achdiawan, H. Kartodihardjo, and A. A. Dewayani (2017). Fire Economy and Actor Network of Forest and Land Fires in Indonesia. *Forest Policy and Economics*, **78**; 21–31

Putra, R., E. Sutriyono, S. Kadir, and I. Iskandar (2019a). Understanding of Fire Distribution in the South Sumatra Peat Area During the Last Two Decades. *GEOMATE Journal*, **16**(54); 146–151

Putra, R., E. Sutriyono, S. Kadir, I. Iskandar, and D. O. Lestari (2019b). Dynamical Link of Peat Fires in South Sumatra and the Climate Modes in the Indo-Pacific Region. *The Indonesian Journal of Geography*, **51**(1); 18–22

Ray, D., D. Nepstad, and P. Moutinho (2005). Micrometeorological and Canopy Controls of Fire Susceptibility in a

Forested Amazon Landscape. *Ecological Applications*, **15**(5); 1664–1678

Saji, N. (2001). Structure of SST and Surface Wind Variability in COADS Observations During IOD Years. *Journal Climate*, **16**; 2735–2751

Saji, N., B. N. Goswami, P. Vinayachandran, and T. Yamagata (1999). A Dipole Mode in the Tropical Indian Ocean. *Nature*, **401**(6751); 360–363

Sastry, N. (2002). Forest Fires, Air Pollution, and Mortality in Southeast Asia. *Demography*, **39**(1); 1–23

Siswanto, S., G. J. van Oldenborgh, G. van der Schrier, R. Jilderda, and B. van den Hurk (2016). Temperature, Extreme Precipitation, and Diurnal Rainfall Changes in the Urbanized Jakarta City During the Past 130 Years. *International Journal of Climatology*, **36**(9); 3207–3225

Stooksbury, D. E., C. D. Idso, and K. G. Hubbard (1999). The Effects of Data Gaps on the Calculated Monthly Mean Maximum and Minimum Temperatures in the Continental United States: A Spatial and Temporal Study. *Journal of Climate*, **12**(5); 1524–1533

Supari, F. Tangang, L. Juneng, and E. Aldrian (2017). Observed Changes in Extreme Temperature and Precipitation Over Indonesia. *International Journal of Climatology*, **37**(4); 1979–1997

Supari, F. Tangang, E. Salimun, E. Aldrian, A. Sopaheluwakan, and L. Juneng (2018). ENSO Modulation of Seasonal Rainfall and Extremes in Indonesia. *Climate Dynamics*, **51**; 2559–2580

Tank, A. M. K., F. W. Zwiers, and X. Zhang (2009). *Guidelines on Analysis of Extremes in a Changing Climate in Support of Informed Decisions for Adaptation*. World Meteorological Organization

Utari, P. A., M. Y. N. Khakim, D. Setiabudidaya, and I. Iskandar (2020). Dynamics of 2015 Positive Indian Ocean Dipole. *Journal of Southern Hemisphere Earth Systems Science*, **69**(1); 75–83

Vincent, L., E. Aguilar, M. Saindou, A. Hassane, G. Jumaux, D. Roy, P. Booneeady, R. Virasami, L. Randriamarolaza, and F. Faniriantsoa (2011). Observed Trends in Indices of Daily and Extreme Temperature and Precipitation for the Countries of the Western Indian Ocean, 1961–2008. *Journal of Geophysical Research: Atmospheres*, **116**(D10); 1–12

Wang, X. L. and Y. Feng (2013). Climate Research Division Atmospheric Science and Technology Directorate Science and Technology Branch, Environment Canada Toronto, Ontario, Canada. *Science and Technology Branch*, **17**; 1–27

Webster, P. J., A. M. Moore, J. P. Loschnigg, and R. R. Leben (1999). Coupled Ocean–Atmosphere Dynamics in the Indian Ocean during 1997–98. *Nature*, **401**(6751); 356–360

WMO (2018). *Guía de Prácticas Climatológicas*. Organización Meteorológica Mundial

Worden, H., M. Deeter, C. Frankenberg, M. George, F. Nichitiu, J. Worden, I. Aben, K. Bowman, C. Clerbaux, and P.-F. Coheur (2013). Decadal Record of Satellite Carbon Monoxide Observations. *Atmospheric Chemistry and Physics*, **13**(2); 837–850

Yamagata, T., S. K. Behera, J.-J. Luo, S. Masson, M. R. Jury, and S. A. Rao (2004). Coupled Ocean-Atmosphere Variability in the Tropical Indian Ocean. *Earth's Climate: The Ocean–Atmosphere Interaction, Geophys. Monogr*, **147**; 189–212

Zhang, F., J. A. Biederman, M. P. Dannenberg, D. Yan, S. C. Reed, and W. K. Smith (2021). Five Decades of Observed Daily Precipitation Reveal Longer and More Variable Drought Events Across Much of the Western United States. *Geophysical Research Letters*, **48**(7); e2020GL092293

Zhang, X., E. Aguilar, S. Sensoy, H. Melkonyan, U. Tagiyeva, N. Ahmed, N. Kutaladze, F. Rahimzadeh, A. Taghipour, and T. Hantosh (2005). Trends in Middle East Climate Extreme Indices from 1950 to 2003. *Journal of Geophysical Research: Atmospheres*, **110**(D22); 1–12

Zhang, X. and F. Yang (2004). RClimDex (1.0) User Manual. *Climate Research Branch Environment Canada*, **22**; 13–14

